

Laser autofluorescent microscopy of histological sections of parenchymatous biological tissues of the dead

O.G. Ushenko¹, A.-V. Syvokorovskaya², V.T. Bachinsky², O.Ya. Vanchuliak², A.V. Dubolazov¹, Yu.O. Ushenko¹, Yu.Ya. Tomka¹, M.L. Kovalchuk¹

¹Chernivtsi National University, 2 Kotsiubynskyi Str., Chernivtsi, Ukraine, 58012

²Bukovinian State Medical University, 3 Theatral Sq., Chernivtsi, Ukraine, 58000

Abstract— The results of experimental testing of the diagnostic capabilities of the method of spectral-selective fluorescence microscopy of temporary necrotic changes in histological sections of kidney internal organs are presented.

Keywords— laser, fluorescence, microscopy, statistical moments, kidney.

I. INTRODUCTION

The results of laser autofluorescence microscopy of the distribution of the intensity of the multidimensional laser autofluorescence (MLA) microscopy of polycrystalline structures [1-3] of biological tissue preparations are presented. The data of a statistical analysis of the distribution of the magnitude of the intensity of MLA networks of biological crystals of histological sections of tissues of the kidney with the parenchymal morphological structure of the dead with different levels of blood loss are presented.

II. FUNCTIONAL DIAGRAM OF MULTIDIMENSIONAL LASER AUTOFLUORESCENCE (MLA) MICROSCOPY OF BIOLOGICAL PREPARATIONS

The multidimensional laser autofluorescence (MLA) microscopy of biological preparations include a next functional block diagram of spectrally selective laser autofluorescence microscopy of parenchymal biological tissues [4-7].

1 – the illumination block IB of biological preparations, which ensures the formation of a polarized laser beam parallel to 2 mm in diameter with a wavelength of 0.405 μm , which excites the intrinsic fluorescence of the fluorophores of biological preparations;

2 – the object block OB is a microscopic table with a two-coordinate movement on which the biological preparation BP is attached;

3 – projection block PB, which with the help of the micro-lens MO (4X) ensures the formation of an autofluorescent microscopic image of a biological preparation BP excited by a laser beam in the plane of the digital camera DC

4 – The block of spectral filtration of BF, which includes the interference light filters F for the spectral selection of the excited autoluminescent polychromatic radiation of an ensemble of BP fluorophores;

5 - a block of photoelectron registration BFR of microscopic fluorescent images of biological preparations BP, which includes the CC and provides the formation of the coordinate digital distribution of the intensity value in the computer interface;

6 – a data processing block DPB that, using a personal computer PC, provides a calculation of the magnitude of the statistical moments of the 1st to 4th orders characterizing the intensity distribution of the spectrally selective autofluorescence of biological preparations BP.

III. SAMPLES

Depending on the level of blood loss (V), the following groups of samples of histological sections of the spleen and kidney with the subsequent level of blood loss were considered:

- $V = 0\text{mm}^3$ - group 1 (20 samples);
- $V = 500\text{mm}^3 \pm 100\text{mm}^3$ - group 2 (22 samples);
- $V = 1000\text{mm}^3 \pm 100\text{mm}^3$ - group 3 (27 samples);
- $V = 1500\text{mm}^3 \pm 100\text{mm}^3$ - group 4 (32 samples);
- $V = 2000\text{mm}^3 \pm 100\text{mm}^3$ - group 5 (22 samples);
- $V = 2500\text{mm}^3 \pm 100\text{mm}^3$ - group 6 (25 samples).

Maps (fragments (1), (3)) and histograms (fragments (2), (4)) distributions of the magnitude of the intensity of MLA polycrystalline structures of samples of histological sections of the kidneys of the dead from group 1 (fragments (1), (2)) and group 3 (fragments (3), (4)), obtained by the method of spectral-selective laser autofluorescence microscopy, are shown in a series of dependences in fig. 1.

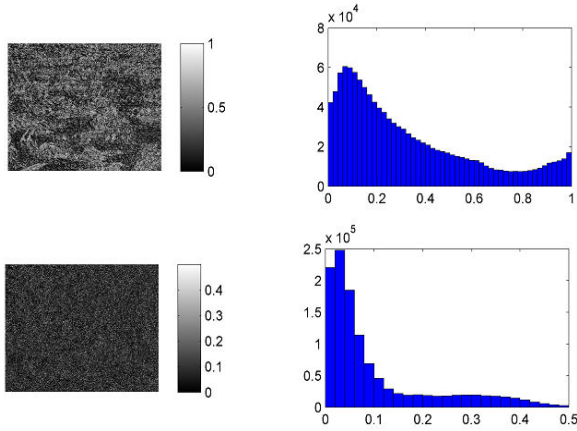


Fig. 1 Maps ((1), (3)) and histograms ((2), (4)) distributions of the autofluorescence intensity of histological sections of the kidney of the control ((1), (2)) and research ((3), (4)) groups the dead

Analysis of the obtained data revealed that with an increase in blood loss and a corresponding decrease in the concentration of blood cells, the fluorescence intensity of the optically anisotropic collagen networks of the kidney of the deceased decreases (Fig. 1, fragments (2), (4)). Such changes are manifested in a decrease in the magnitudes of the corresponding statistical parameters — the mean and variance, which characterize the distribution of the intensity of the MLA of histological sections of the kidney tissue of all groups of the dead. In parallel with this, the magnitudes of the 3rd and 4th order statistical moments, which characterize the asymmetry and excess of distributions of the corresponding MLA histological sections of the kidney of the dead in the range of blood loss $0 \text{ mm}^3 \div 2500 \text{ mm}^3$, increase.

The data of statistical analysis of changes in the structure of MLA samples of histological sections of the kidney of the dead with varying degrees of blood loss illustrate the statistical moments of the 1st - 4th orders, the magnitudes of which are shown in table 1.

Table 1 Statistical structure of autofluorescence intensity maps of histological sections of the kidney of the dead with varying degrees of blood loss

| Blood loss, mm^3 | 0 | $500 \pm 100 \text{ mm}^3$ | $1000 \pm 100 \text{ mm}^3$ |
|---------------------------|-----------------------------|-----------------------------|-----------------------------|
| The average, SM_1 | 0.32 ± 0.013 | 0.26 ± 0.012 | 0.21 ± 0.011 |
| Criteria, t, p | $p < 0.05$ | $p < 0.05$ | $p < 0.05$ |
| Dispersion, SM_2 | 0.26 ± 0.012 | 0.21 ± 0.011 | 0.16 ± 0.07 |
| Criteria, t, p | $p < 0.05$ | $p < 0.05$ | $p < 0.05$ |
| Asymmetry, SM_3 | 0.97 ± 0.045 | 1.33 ± 0.062 | 1.61 ± 0.074 |
| Criteria, t, p | $p < 0.05$ | $p < 0.05$ | $p < 0.05$ |
| Excess, SM_4 | 0.51 ± 0.022 | 1.04 ± 0.043 | 1.69 ± 0.078 |
| Criteria, t, p | $p < 0.05$ | $p < 0.05$ | $p < 0.05$ |
| Blood loss, mm^3 | $1500 \pm 100 \text{ mm}^3$ | $2000 \pm 100 \text{ mm}^3$ | $2500 \pm 100 \text{ mm}^3$ |
| The average, SM_1 | 0.16 ± 0.007 | 0.09 ± 0.004 | 0.04 ± 0.002 |
| Criteria, t, p | $p < 0.05$ | $p < 0.05$ | $p < 0.05$ |
| Dispersion, SM_2 | 0.11 ± 0.005 | 0.07 ± 0.003 | 0.03 ± 0.001 |
| Criteria, t, p | $p < 0.05$ | $p < 0.05$ | $p < 0.05$ |
| Asymmetry, SM_3 | 1.92 ± 0.089 | 2.23 ± 0.11 | 2.51 ± 0.12 |
| Criteria, t, p | $p < 0.05$ | $p < 0.05$ | $p < 0.05$ |
| Excess, SM_4 | 2.02 ± 0.096 | 2.43 ± 0.11 | 2.89 ± 0.13 |
| Criteria, t, p | $p < 0.05$ | $p < 0.05$ | $p < 0.05$ |

Established:

- the range of changes in the magnitude of the 1st to 4th order statistical moments, characterizing the distribution of the intensity of the MLA of histological sections of the

kidney, in terms of the volume of blood loss is $0 \text{ mm}^3 \div 2500 \text{ mm}^3$;

- the statistical moment of the 1st order SM_1 changes within the range of variation of averages magnitudes from 0.32 to 0.04;
- the statistical moment of the 2nd order SM_2 changes within the range of variation of averages magnitudes from 0.26 to 0.03;
- the statistical moment of the 3rd order SM_3 changes within the range of variation of averages magnitudes from 0.97 to 2.51;
- the statistical moment of the 4th order SM_4 changes within the range of variation of averages magnitudes from 0.51 to 2.89.

In fig. 2 shows diagrams of changes in the set of statistical moments of the 1st - 4th orders $SM_{1;2;3;4}$, which characterize the coordinate structure of the distributions of random laser autofluorescence intensity (MLA) values of optically anisotropic collagen networks of a set of histological sections of the kidney of the dead from all groups according to the level of blood loss.

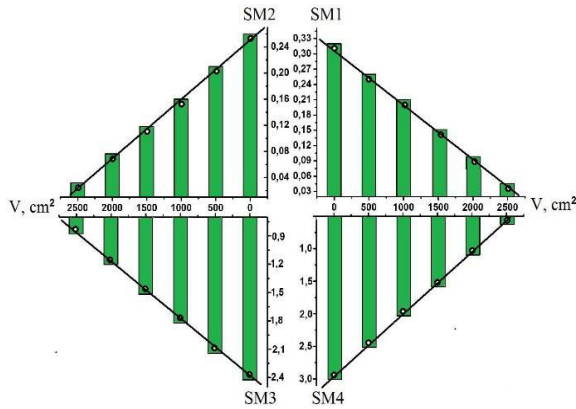


Fig. 2 Dependences of the magnitude of the average (1), dispersion (2), asymmetry (3) and excess (4), which characterize the autofluorescence intensity maps of histological sections of the kidney of the deceased with varying degrees of blood loss.

Table 2 Accuracy of determining the volume of blood loss in the kidney

| Blood loss, mm^3 | $500 \pm 100 \text{ mm}^3$ | $1000 \pm 100 \text{ mm}^3$ | $1500 \pm 100 \text{ mm}^3$ | $2000 \pm 100 \text{ mm}^3$ | $2500 \pm 100 \text{ mm}^3$ |
|---------------------------|----------------------------|-----------------------------|-----------------------------|-----------------------------|-----------------------------|
| Average, SM_1 | 96 | 96 | 96 | 94 | 94 |
| Dispersion, SM_2 | 96 | 96 | 94 | 92 | 92 |
| Asymmetry, SM_3 | 84 | 86 | 86 | 86 | 84 |
| Excess, SM_4 | 94 | 94 | 92 | 90 | 90 |

Statistical analysis of laser spectral-selective laser autofluorescence microscopy of optically anisotropic grids of biological crystals found (Fig. 2, Table 1) a decrease in average, dispersion, and, conversely, an increase in asymmetry and excess, which characterize the distributions of the intensity of MLA of histological sections of the kidney of the deceased, within volume of blood loss $0 \text{ mm}^3 \div 2500 \text{ mm}^3$. The most sensitive to changes in the fluorescence intensity of histological sections of the kidney with blood loss of varying volume were the statistical moments of the 1st, 2nd, and 4th orders.

IV. THE EFFECTIVENESS OF THE DIFFERENTIAL DIAGNOSIS OF THE DEGREE OF BLOOD LOSS BY LASER AUTOFLUORESCENCE MICROSCOPY

For each statistical moment that characterizes the distribution of the MLA intensity values of a set of spleen samples from different groups of deceased, the accuracy of determining the blood loss volume was found on the basis of a series of nomograms presented in fig. 3.

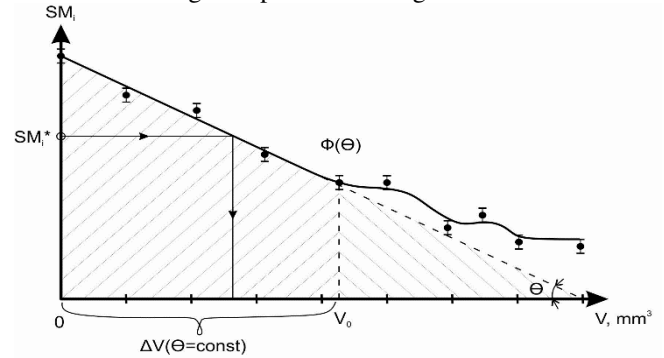


Fig. 3 Analytical scheme for determining the volume of blood loss of the dead according to the method of laser autofluorescence microscopy.

The analysis of the obtained data revealed the following parameters of the diagnostic efficiency of the statistical analysis of the results of the method of spectrally selective laser autofluorescence microscopy of histological sections of parenchymal biological tissues:

1. For all studied biological preparations, the range of sensitivity of the method of spectral-selective laser autofluorescence microscopy to changes in the volume of blood loss of the dead is the maximum level $0 \text{ mm}^3 \div 2500 \text{ mm}^3$.

2. The accuracy of the method of spectral-selective laser autofluorescence microscopy of biological samples varies in the range:

- $\Delta V = 0 \text{ mm}^3 \div 2500 \text{ mm}^3 \Leftrightarrow 86\% - 92\%$;

3. The maximum level is reached for the following statistical parameters characterizing laser autofluorescence maps of histological sections of the kidney -

$$\begin{cases} SM_1 \Leftrightarrow 94\% - 96\%; \\ SM_2 \Leftrightarrow 94\% - 96\%; \\ SM_4 \Leftrightarrow 90\% - 94\%. \end{cases}$$

V. CONCLUSIONS

1. A set of maps and histograms of random fluorescence intensity distributions of blood corpuscles of the polycrystalline component of histological sections of parenchymal biological tissues of the spleen and kidney of the deceased with varying degrees of blood loss were studied using spectral-selective laser autofluorescence microscopy.

2. The dynamics of changes in the magnitude of the statistical moments of the 1st - 4th orders, characterizing the distribution of MLA histological sections of parenchymal (spleen, kidney) tissues of the deceased with different blood loss - $\Delta V = 0 \text{ mm}^3 \div 2500 \text{ mm}^3$, was studied.

3. The magnitudes and ranges of accuracy of the method of spectral-selective laser autofluorescent microscopy of biological preparations of the spleen are determined -

$$\begin{cases} SM_1 \Leftrightarrow 94\% - 96\%; \\ SM_2 \Leftrightarrow 94\% - 96\%; \\ SM_4 \Leftrightarrow 90\% - 94\%. \end{cases}$$

CONFLICT OF INTEREST

The authors declare that they have no conflict of interest.

REFERENCES

1. Ushenko, A.G., Dubolazov, A.V., Ushenko, V.A., Novakovskaya, O.Y. Statistical analysis of polarization-inhomogeneous Fourier spectra of laser radiation scattered by human skin in the tasks of differentiation of benign and malignant formations (2016) *Journal of Biomedical Optics*, 21 (7), 071110.
2. Ushenko, Y.A., Dubolazov, A.V., Angelsky, A.P., Sidor, M.I., Bodnar, G.B., Koval, G., Zabolotna, N.I., Smolarz, A., Junisbekov, M.S. Laser polarization fluorescence of the networks of optically anisotropic biological crystals (2013) *Proceedings of SPIE - The International Society for Optical Engineering*, 8698, 869809.
3. Ushenko, Yu.A., Bachynsky, V.T., Vanchulyak, O.Ya., Dubolazov, A.V., Garazdyuk, M.S., Ushenko, V.A. Jones-matrix mapping of complex degree of mutual anisotropy of birefringent protein networks during the differentiation of myocardium necrotic changes (2016) *Applied Optics*, 55 (12), pp. B113-B119.
4. Ushenko, Yu.A., Dubolazov, A.V., Karachevtcev, A.O., Zabolotna, N.I. A fractal and statistic analysis of Mueller-matrix images of phase inhomogeneous layers (2011) *Proceedings of SPIE - The International Society for Optical Engineering*, 8134, 81340P.
5. Dubolazov, A.V., Pashkovskaya, N.V., Ushenko, Yu.A., Marchuk, Yu.F., Ushenko, V.A., Novakovskaya, O.Yu. Birefringence images of polycrystalline films of human urine in early diagnostics of kidney pathology (2016) *Applied Optics*, 55 (12), pp. B85-B90.
6. Dubolazov, A.V., Koval, G.D., Zabolotna, N.I., Pavlov, S.V. Fractal structure of optical anisotropy Mueller-matrices images of biological layers (2013) *Proceedings of SPIE - The International Society for Optical Engineering*, 9066, 90661W.
7. Ushenko, V.A., Sidor, M.I., Marchuk, Yu.F., Pashkovskaya, N.V., Andreichuk, D.R. Azimuth-invariant mueller-matrix differentiation of the optical anisotropy of biological tissues (2014) *Optics and Spectroscopy (English translation of Optika i Spektroskopiya)*, 117 (1), pp. 152-157.

Use macro [author address] to enter the address of the corresponding author:

Author: Alexander Ushenko
 Institute: Chernivtsi National University
 Street: 2 Kotsyubinskogo Str.
 City: Chernivtsi
 Country: Ukraine
 Email: o.ushenko@chnu.edu.ua